ELSEVIER

Ceramics International 31 (2005) 897–904

CERAMICS INTERNATIONAL

www.elsevier.com/locate/ceramint

Post mortem study of Al_2O_3/SiC/C/$MgAl_2O_4$ ceramic lining used in torpedo cars

Sérgio Murilo Justus[a], Sidiney Nascimento Silva[b], Fernando Vernilli Jr.[c,*], Alex Mazine[b], Reginaldo Gomes Toledo[b], Ricardo Magnani Andrade[a], Oscar Rosa Marques[b], Elson Longo[a], João Baptista Baldo[a], José Arana Varela[a]

[a]*Multidisciplinary Center for Development of Ceramic Materials, CMDMC/UFSCar, São Paulo, Brazil*
[b]*Companhia Siderúrgica Nacional, CSN, Rio de Janeiro, Brazil*
[c]*Materials Engineering Department, Faenquil, São Paulo, Brazil*

Received 28 June 2004; received in revised form 23 August 2004; accepted 28 September 2004
Available online 21 January 2005

Abstract

A post mortem study of Al_2O_3/SiC/C/$MgAl_2O_4$ (ASCMg) refractory lining used in Companhia Siderurgica Nacional (CSN) torpedo car was conducted in order to determine the corrosion equation developed during industrial application. Different samples were collected and characterized using the following techniques: Chemical Analysis by X-Ray Fluorescence, Thermal-Gravimeter and Differential Thermal Analysis (TG–DTA), Mercury Porosimetry, Helium Picnometry, Dilatometry, X-Ray Diffractometry, Scanning Electronic Microscopy (SEM) and Energy Dispersive Scanning (EDS). It was found that slag containing a high amount of calcium aluminum silicate interacts with refractory microstructure causing corrosion. From this effect it is noted the introduction of an alkaline incorporating concurrent mechanism, in addition to corundum being turned into β-alumina and the oxidation of SiC through Na_2O resulting in better protective conditions to graphite, thereby improving refractory lining shelf life.

Keywords: C. Corrosion; E. Refractory; Torpedo car

1. Introduction

It has been common practice in Brazil, among coke integrated steel mills, to run blast furnaces in such a way as to reduce as much as possible sulfur content in hot metal, which entails higher volume and lower slag basicity, higher reductant consumption and lower blast furnace output.

However, in view of stiff competitiveness brought about by a new and globalized marketplace, this practice has changed, as the newly-installed blast furnaces must satisfy the amount of hot metal required by the BOF shops, so as to enable an increase in productivity.

In this way, a new approach to cut down on operational costs, while raising BF productivity has been introduced in the integrated steel mills, aimed at transferring the bulk of sulfur removal to external desulfurization process [1].

In view of new guidelines, aimed at bolstering productivity, it is of paramount importance to develop new techniques to preclude torpedo car refractory lining corrosion, with new alternatives to hot metal refining pre-treatment to satisfy productivity increase, without losing sight of steel internal quality requirements.

Lee et al. [2–4] studied the microstructures, penetration and dissolution mechanisms of Al_2O_3/SiO_2/SiC/C refractory matrices with aluminum, silicon, Si_3N_4, BN, B_2O_3 and B_4C additives. Lee showed that the carbon content dominates the resistance to CaO–MgO–Al_2O_3–SiO_2 slag penetration, while the viscosity of liquid phases present has a significant influence when the matrix carbon contents are similar. Silicon and Si_3N_4 additives reduce slag penetration resistance because of indirect oxidation of carbon to form

* Corresponding author.
E-mail address: vernilli@demar.faenquil.br (F. Vernilli Jr.).

0272-8842/$30.00
doi:10.1016/j.ceramint.2004.09.016

SiC. B_4C, in particular, and B_2O_3 also reduce slag penetration resistance because of formation of a more fluid boron-contain liquid, while aluminum and BN addition have to significant effect. Carbon and BN hardly react with the slag, while SiC partially reacts with it, leading to deposition of carbon as a dense layer. Corundum present in the refractories also readily dissolves in the slag. Microstructurally, slag penetration resistance is associated with the dense carbon layer located at the slag-refractory interface.

Resende et al. [5] studied the behavior of alumina/magnesia/carbon (AMC) refractories, by using different kinds of aggregates for different carbon concentrations.

Different slag compositions were used, the binary basicity (CaO/SiO_2) was changed and scorification tests through dynamic method were conducted to assess the influence of alumina, carbon, magnesia and silica contents over the formulations developed.

As a result of the studies, it was found that higher graphite concentrations in the matrix lead to better corrosion resistance by slag attack and better thermo–mechanical properties, due to their excellent thermal conductivity, high refractability and low wettability by slag.

Lower concentration in the mullite phase microstructure is desired, as it leads to lower calcium alumino–silicate production, which accounts for the formation of eutetic anorthite-gehlenite-pseudowollastonite at about 1265 °C, resulting in a lower wear because of thermoclase structural effect.

High periclase/mullite phase relations lead to high mullite consumption, because of its reaction with periclase, producing forsterite and alumina.

This highly reactive precipitated alumina is able to combine with the periclase surplus, thus forming initially magnesium aluminate and further magnesium aluminum spinel.

The combined effect of such reactions in the refractory microstructure causes the formation of barriers in the open porosity, resulting in the generation of concurrent protective mechanisms.

This study aims to settle the corrosion mechanism involved in the refractory system based on alumina/silicon carbide/magnesium aluminum spinel used as torpedo car refractory lining.

2. Materials and methods

At the end of refractory lining life of CSN #8 torpedo car, samples from five different areas were collected, namely: slag line, ceramic pad, cone, dome and central cylinder. In the following work surface distances, 0 (work face), 50, 100 mm and unused material these samples, along with the samples of this lining, prior to use, were characterized by Chemical Analysis (ICP/AES), Differential and Gravimetric Thermal Analysis, Mercury Porosimetry, Helium Picnometry, X-ray Diffractometry and Scanning Electronic Microscopy (SEM) coupled with Energy Dispersive Scanning (EDS) so as to determinate the service corrosion mechanism of this refractory.

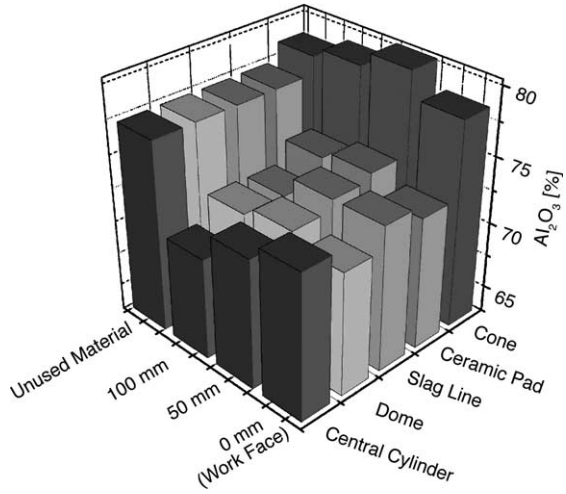

Fig. 1. Chemical analysis of alumina for different depths.

3. Results and discussion

3.1. Chemical analysis

Analyses of aluminum oxide contents for different depths suggest hardly any change in composition. However, a bigger alumina composition difference was found in the sample collected from the cone, Fig. 1 between hot side and the 50 mm area, pointing to higher microstructure consumption by the hot metal/slag bath.

This effect is explained by the fact that the material used in the cone is the conventional line of ASC refractory, consisting of mullite in the matrix, free from aluminum magnesium spinel, which causes a bigger matrix wear through production of low density phases based upon calcium aluminum silicates.

The highest SiO_2, Fe total contents and CaO (particularly at a 50 mm depth) were again found for the sample collected from the cone, Fig. 2 indicating to hot metal/slag bath penetration, because of mullite presence in the refractory matrix.

Barely any variation in the MgO contents was noticed, Fig. 3 most likely due to the fact that magnesium oxide is combined as $MgAl_2O_4$. This is a phase of high refractoriness and amphoteric nature, leading to a higher corrosion resistance, as it will be discussed later in the X-ray diffraction studies.

Higher Na_2O contents can be found, as hot side is approached. Such an effect is due to Na_2O presence in the atmosphere and torpedo car bath. The reason for this alkaline compound is the raw materials, which make up BF burden (coke, sinter, iron ore, etc.) as well the presence of

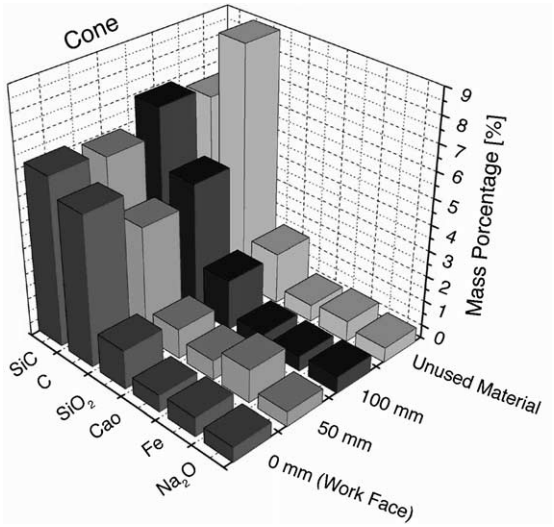

Fig. 2. Chemical analysis of cone for different depths.

aluminum sludge, used as a source of metallic aluminum to make up the desulfurizing agents in the Desulfuration Station of CSN (CaO/aluminum sludge and CaC_2/CaO/$CaCO_3$/Al).

The lower contents of silicon carbide and carbon found in the 50 mm area compared to the 0 mm (work face) area are because of carbon and silicon carbide oxidation mechanisms which are prevalent in refractory inner and hot side, according to the following equations [6–8]:

Refractory work side:

$$C_{(s)} + \frac{1}{2}O_2 \rightarrow CO \quad (1)$$

$$C_{(s)} + Na_2O \rightarrow CO + Na_{2(g)} \quad (2)$$

$$Na_2 + \frac{1}{2}O_{2(g)} \rightarrow Na_2O \quad (3)$$

Inner side:

$$SiC_{(s)} + CO \rightarrow SiO_{(g)} + 2C \quad (4)$$

$$SiO_{(g)} + CO \rightarrow SiO_{2(s)} + C \quad (5)$$

$$SiC_{(s)} + Na_2O \rightarrow SiO_{(g)} + Na_{2(g)} + C \quad (6)$$

$$SiO_{(g)} + Na_2O \rightarrow SiO_{2(s)} + Na_{2(g)} \quad (7)$$

3.2. Thermal gravimetric and differential analysis

The aforesaid oxidation mechanisms are corroborated by differential and gravimetric analysis studies, which point to higher SiC concentration on the work side (0 mm), as illustrated in the ATG curves (Fig. 4) showing a significant difference in the values of mass loss of the 0 mm area samples, compared with the 50 mm area at about 800 and 1000 °C (initial temperature for SiC oxidation). After 1000 °C, mass fluctuation was stabilized followed by gain. This effect is explained by the mass balance from SiC decomposition, followed by SiO_2 precipitation (ratio SiO_2/SiC = 1.50).

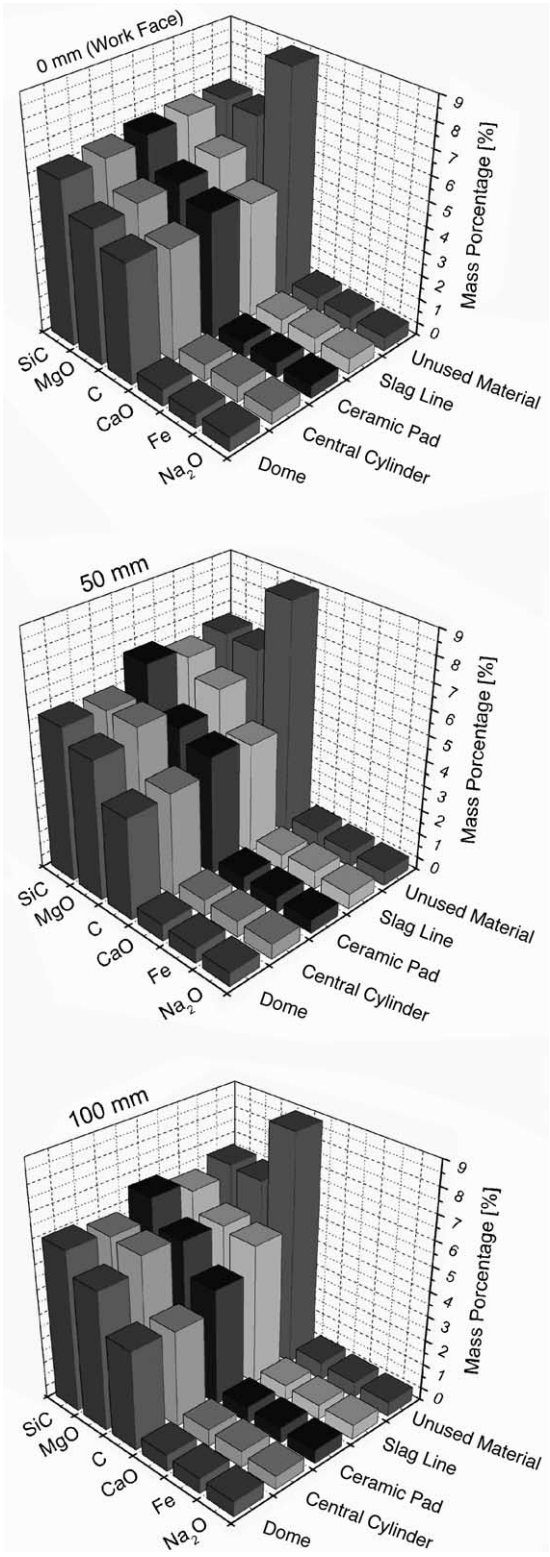

Fig. 3. Chemical analysis of refractories for different depths.

ATG curve evaluations from unused material samples of refractory show, on average, an initial mass loss of 4.4% up to 500 °C, followed by 4.0% loss for the 500–800 °C interval. The first interval is related to evolution of the

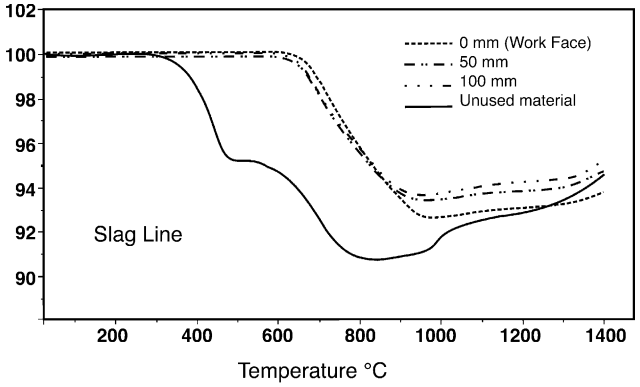

Fig. 4. Typical gravimetric thermal analysis from samples studied in accordance with the depth.

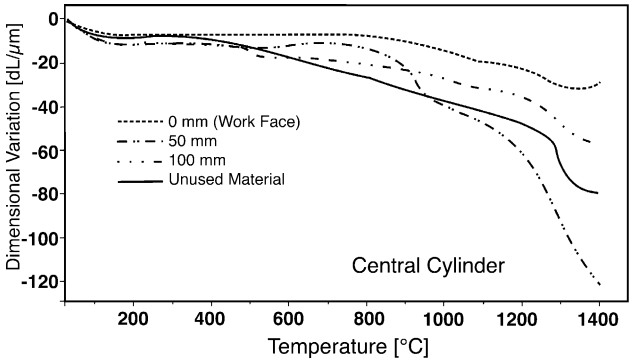

Fig. 6. Typical dilatometric curves from samples in connection with post mortem study.

binding system solvent (phenolic resin), while the second interval is essentially related to fixed carbon oxidation.

It should be noted that during the unused material heating there is the reaction of metallic aluminum, which is intrinsic to material with nitrogen and carbon. Initially, as reaction products AlN and Al_4C_3 are, respectively obtained. In the second step, both reaction products are converted into Al_2O_3, by means of carbon monoxide oxidation [9].

Differential thermal analysis, Fig. 5 shows the unused material with an endothermic peak at around 650 °C, corroborated by X-ray diffraction studies and the literature [9,10] as being AIN phase.

3.3. Dilatometry

Ambient temperature dilatometric studies at torpedo car working temperature (1400 °C) were conducted as shown in Fig. 6.

Fig. 6 analyses suggest temperatures hovering around 850–900 °C, strong expansion, as shown in the dilatometric curves at 50 mm depth. Pursuant to literature information [11], at 873 °C, there is a reconstructive transformation of high quartz into high tridymite. Assuming a quartz density of 2.65 g cm^{-3} and a tridymite density of 2.26 g cm^{-3}, there will be a volumetric expansion of 17% during transformation.

Pursuant to the oxidation mechanisms mentioned earlier inside refractory (50 mm area) there will be an oxidation, notably of SiC, resulting in silica precipitation, which accounts for expansion during the reconstructive transformation mentioned earlier.

3.4. Mercury porosimetry and helium picnometry

Fig. 7 illustrates the mercury porosimetry and helium picnometry results for different samples investigated. Result analyses point to higher values for the actual density in the 50 mm area, indicating the production of new phases of higher actual density. Such results are in keeping with the statements regarding mass balance from SiC decomposition followed by SiO_2 precipitation.

The highest apparent density and structural density values toward hot side are due to pores being filled up by hot metal/slag bath. Fig. 8 analyses point to, on average, an apparent porosity increase from 6.0 (unused material) to 12 vol.% (100 mm from work face), as refractories are put

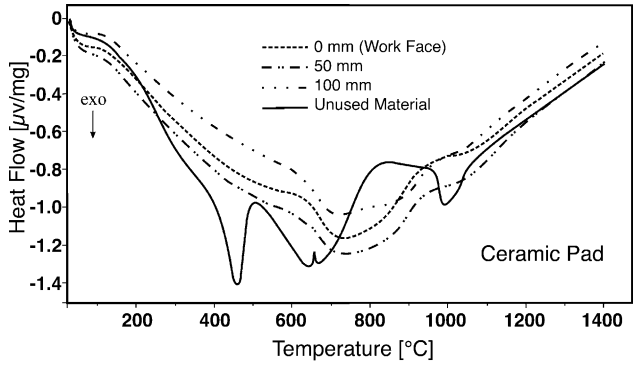

Fig. 5. Typical differential thermal analysis from samples studied in accordance with the depth.

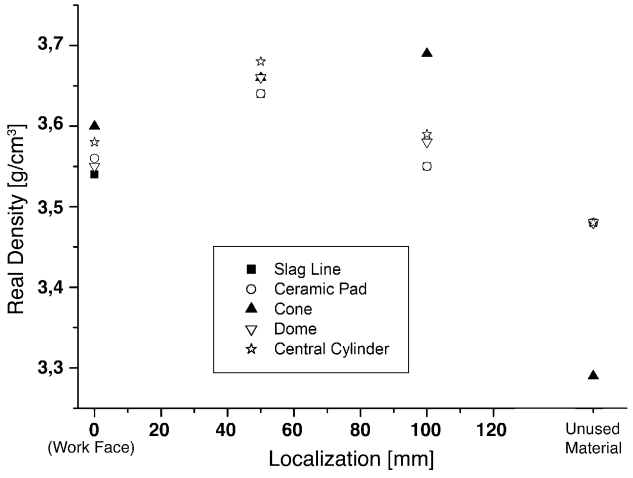

Fig. 7. Actual density according to the depth studied in five areas.

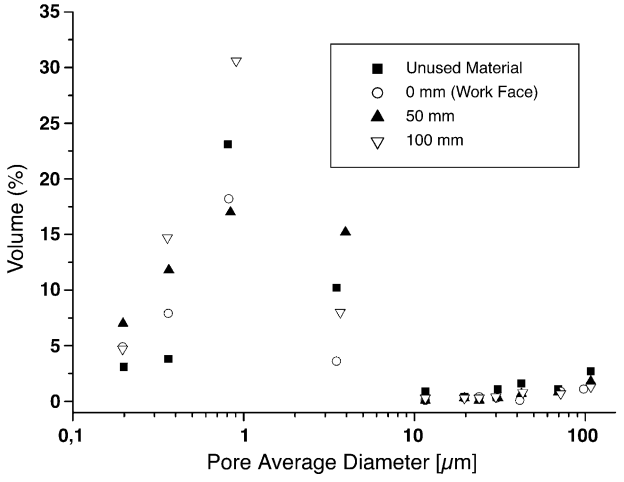

Fig. 8. Pore size distribution of post mortem study samples.

into service. Apparent porosity evaluations, for the depth studied, reveal a slight reduction in the apparent porosity, as the work side is approached. This is explained by the fact of the open porosity being filled up by microstructure oxidation products (SiC, C, AlN, Al_4C_3) as well as by hot metal/slag penetration.

Evaluations of accumulated and incremental pore size distribution for different areas of depth indicate size pore percentage increase from 3 to 5 mm for the 50 mm deep area from the hot face. Such results are to be ascribed to SiC and C oxidation, resulting in refractory microstructure permeability being augmented.

Fig. 9 shows a pore average diameter for different areas, indicating an augmentation of pore average diameter 50 mm deep from hot side, followed by a decrease as 100 mm deep is approached.

It was found that the ASCMg based refractory composition initially presents (new material) an average smaller pore diameter when compared to ASC conventional system, thus reflecting a lower permeability to fluids stemming from atmosphere and torpedo car bath, and therefore, a lower wear rate.

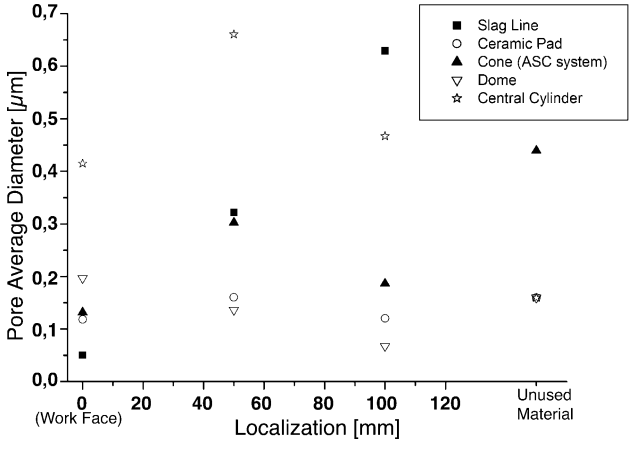

Fig. 9. Average pore diameter of samples related to post mortem study.

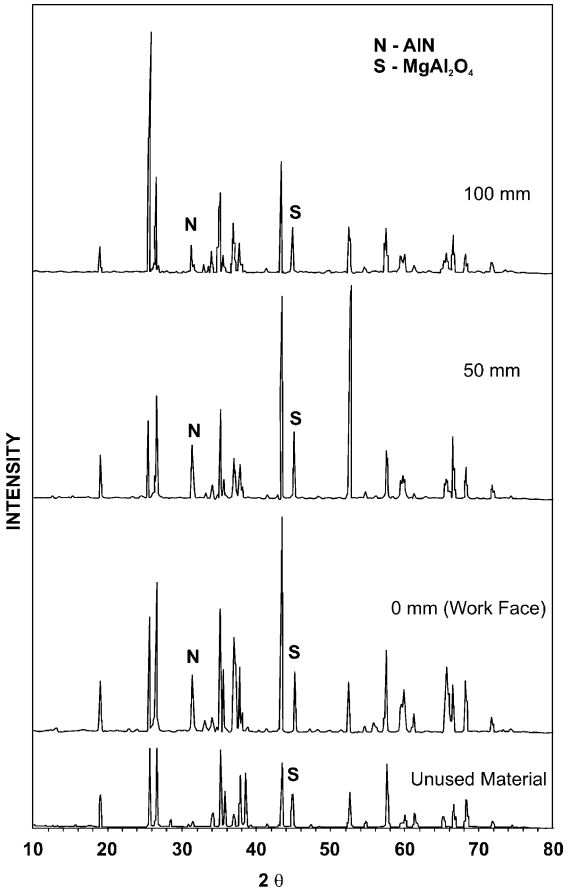

Fig. 10. X-ray diffraction in the post mortem study samples across the depth.

3.5. X-ray diffraction

X-ray diffraction examinations were carried out in the samples, so as to gauge mineralogical development across the depth for each of the selected areas, Fig. 10.

AIN formation was detected in the post mortem study samples, Fig. 10. Such results were corroborated by differential thermal analysis studies from fresh samples, which again showed an endothermical peak at about 650 °C.

The presence of this phase is owing to the reaction of $Al_{(l)}$ with $N_{2(g)}$. Further, $AlN_{(s)}$ is turned into Al_2O_3 as described in the equation below:

$$Al_{(l)} + \frac{1}{2}N_{2(g)} \rightarrow AlN_{(s)}, \quad (8)$$

$$2AlN_{(s)} + 3CO \rightarrow Al_2O_3 + N_{2(g)} + 3C. \quad (9)$$

As a result, AIN precipitation is obtained in the open porosity, followed by Al_2O_3 and carbon formation, by means of CO consumption, thereby, strengthening refractory bonding system, as well creating barriers in the open porosity, a stumbling block to percolation of fluids stemming from atmosphere and torpedo car bath.

Evaluations from ASCMg refractory samples indicate a shift from $MgAl_2O_4$ phase peak to figures greater than 2θ for

Table 1
Mineralogical composition and $MgAl_2O_4$ crystal structure prior to and post alkaline attack compared to phases stemming from $MgAl_2O_4$ and arising out of post mortem study refractories

Situation	Mineralogical composition	Crystal structure
Prior alkaline attack	$MgAl_2O_4$	Cubic
Post alkaline attack	$Na_2MgAl_{10}O_{17}$; $Na_{1,67}Mg_{0.67}Al_{10,33}O_{17}$	Rhombohedra (Hexagonal)
Derivate phases of $MgAl_2O_4$ from post mortem study refractories	Mg–Al–O	Monoclinic
	$NaMg_2Al_{15}O_{25}$	Hexagonal

all areas studied, except for the cone sample, whose conventional lining is ASC based free from $MgAl_2O_4$. This effect is more clearly noticed on the work side (0 mm) and less conspicuous as one walks toward material cold side.

This result, coupled with higher alkali contents in the 0 and 50 mm areas and further validated by Scanning Electronic Microscopy coupled with EDS, points to Mg–Al–O phase formation, followed by phase $NaMg_2Al_{15}O_{25}$ production.

In order to confirm sodium combination with $MgAl_2O_4$ phase, a blend $MgAl_2O_4$:Na_2CO_3 was prepared, weight ratio 1:1, by using magnesium aluminum spinel utilized in the ASCMg refractory matrix, followed by heating up to torpedo car operating average temperature (1400 °C) and kept for 6 h under normal atmosphere, followed by furnace natural cooling. The sample was prepared for characterization by X-ray diffraction and the phases described on Table 1 were obtained.

As reaction products, phases with higher sodium molar fraction were obtained when compared with the phase from post mortem study. Such a fact is explained by the severity of alkaline attack test, using 50% in weight of Na_2CO_3. However, such results corroborate the possibility of forming sodium–magnesium aluminates from spinel structure.

As a result, mullite phase replacement by aluminum magnesium spinel phase of refractory lining, in addition to eliminating matrix wear through calcium aluminum silicates (eutectic anorthite-gehlenite-pseudowollastonite: 1265 °C) [12] it enables the creation of an alkaline incorporating concurrent mechanism, in addition to the transformation of corundum into beta alumina and SiC oxidation through Na_2O [5], which leads to a higher graphite protection.

3.6. Scanning electronic microscopy (SEM) coupled with energy dispersive scanning (EDS)

Dome samples were selected for SEM/EDS study and confirmed by X-ray diffraction findings.

Fig. 11 shows the composition image of the area at 0 mm (work face) under microstructure global view (a), further detailing in other micrographies shown by arrows (b).

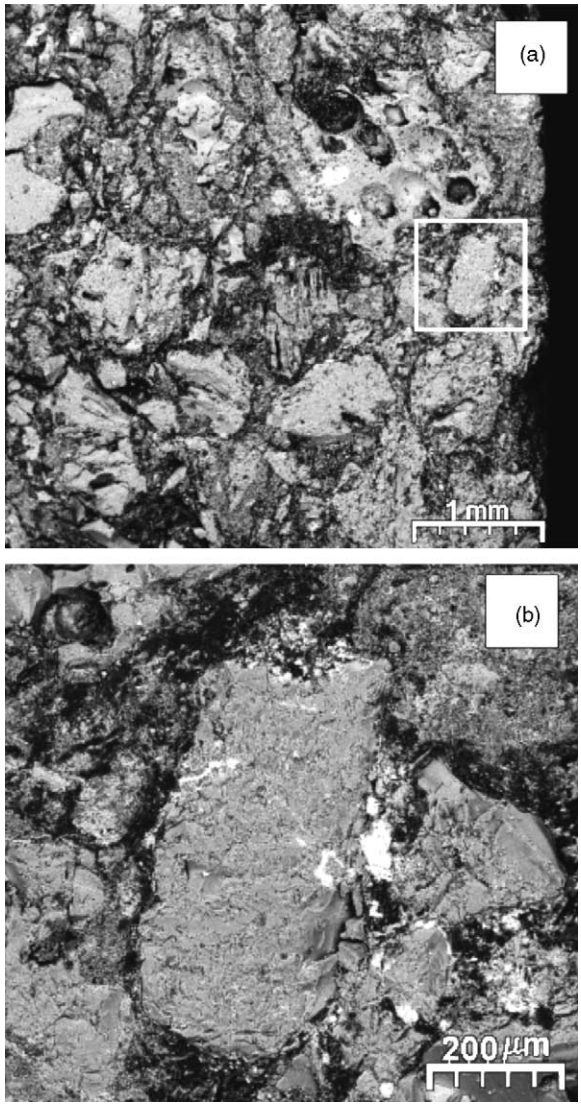

Fig. 11. SEM images from refractory collected at torped car dome area: (a) global view, (b) detail of $MgAl_2O_4$ grain, demarcated area on (a).

It was found that the $MgAl_2O_4$ grain shown in Fig. 11(a) was slightly changed, as a result of slag influence, working as a barrier to corrosion.

Further tests by using EDS made it possible qualitative composition detailing as well as distribution of the main elements, which make up Fig. 11 composition image, by means of X-ray mapping of those elements identified from EDS, Fig. 12.

In addition to the main intrinsic elements, which make up the material (Al, Si, C, Mg, O, Ti), a strong counting intensity for sodium line as noted X-ray mapping stemming from microanalysis suggests the coexistence of Na, Mg, Al and O, thereby, corroborating X-ray diffraction results which lead to the transformation of $MgAl_2O_4$ phase crystalline grating toward Mg–Al–O and $NaMg_2Al_{15}O_{25}$ phases, resulting in graphite protection, according to carbon and Na map comparison shown in Fig. 12.

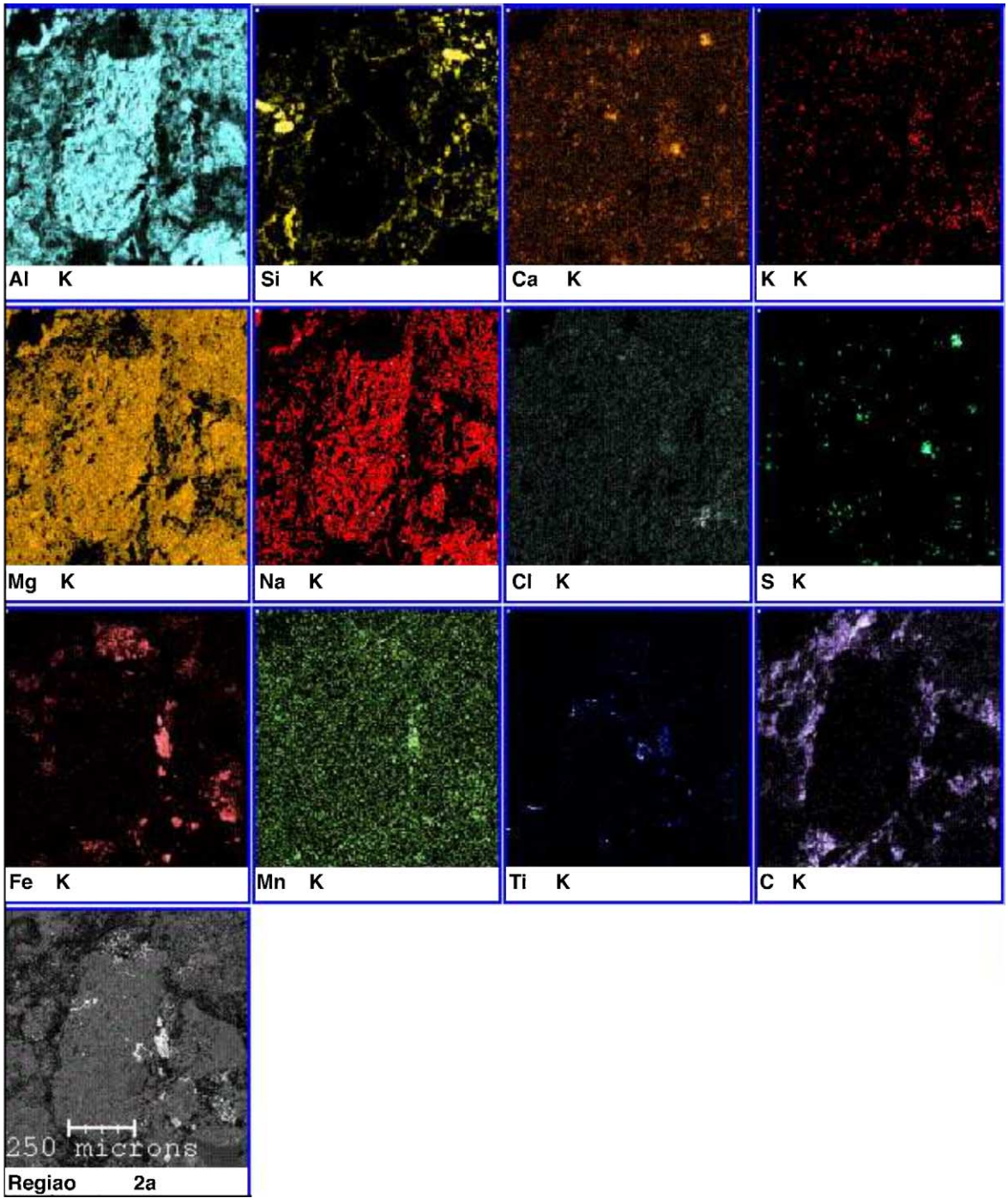

Fig. 12. EDS mapping of work face dome shown in Fig. 11(b).

4. Conclusion

The replacement of conventional ASC refractory lining in the slag line and impact zone areas by ASCMg refractories free from mullite, enabled CSN torpedo car life from 250 to 400 thousand metric tons of hot metal transported, as long as CaO/aluminum sludge blend was being used, with an average desulfurization rate of 55%.

Nevertheless, with aluminum sludge content increase in the blend from 6 to 10% as of April/98, along with the use of new $CaC_2/CaCO_3/CaO/Al$ based desulfurizing agents, coupled with a rise in the desulfurization rate to 80%, led to lining premature wear and more repair so as to ensure a 400 thousand ton campaign of hot metal.

In view of the results, obtained from the post mortem study of ASCMg refractory lining used in #8 torpedo car, the following can be concluded:

Calcium alumino silicate-rich slag consisting of ground alkaline element fractions intrinsic to blast furnace raw materials and arising out of the desulfurizing blends used (aluminum sludge – Al source) interacts with refractory microstructure, thus leading to SiC oxidation through the $Na_2O_{(l)}$ effect, resulting in $SiO_{2(s)}$ precipitation.

The $Na_{2(g)}$, which is produced is not volatilized and is quickly oxidized in the torped car atmosphere, there by forming $Na_2O_{(s)}$, which will precipitate in bath and become $Na_2O_{(l)}$ liquid.

A portion of $Na_2O_{(l)}$ stemming from the oxidation mechanism and alkaline recirculation will combine with the magnesium aluminum spinel phase, leading to reactions initially to Mg–Al–O phase formation followed by $NaMg_2Al_{15}O_{25}$. As a result of this effect, one can notice the introduction of alkaline incorporating concurrent mechanism, in addition to the transformation of corundum into beta alumina and SiC oxidation by Na_2O, thus resulting in graphite higher protection and longer refractory lining life.

Such statements are validated by X-ray diffraction studies and corroborated by microanalyses using EDS, which point to a preferred coexistence of Na with Mg, Al and O over carbon.

$MgAl_2O_4$ grain located close to refractory lining work side taken from arch suggests a slight change, as a result of slag action, working as a barrier to corrosion.

Acknowledgements

The authors are grateful to Companhia Siderúrgica Nacional, Saint-Gobain, FAPESP, FINEP/PRONEX and CNPq for their competent and active support in all aspects of this work.

References

[1] J. Finardi, et al. International Conference of Dessulfuration and Inclusions Control, Associação Brasileira de Metais, Volta Redonda - RJ, October, 1997, pp. 19–90.
[2] C.F. Chan, B.B. Argent, W.E. Lee, J. Am. Ceram. Soc. 81 (12) (1998) 3177–3188.
[3] W.E. Lee, S. Zhang, Int. Mater. Rev. 44 (3) (1999) 77–104.
[4] C.F. Chan, B.B. Argent, W.E. Lee, Calphad (Computer Coupling of Phase Diagrams and Thermochemistry) 27 (1) (2003) 115–125.
[5] W.S. Resende, et al. J. Eur. Ceram. Soc. (January 2000) 1–7.
[6] A. Yamaguchi, Behaviors of SiC and Al added to carbon-containing refractories, Taikabutsu Overseas 4 (3) (1984) 14–18.
[7] H. Kyoden, et al. Taikabutsu 37 (12) (1985) 719.
[8] H. Kyoden, et al. Taikabutsu Overseas 7 (2) (1987) 24–33.
[9] G. Correa UFSCar, 1990. Ph. D. Thesis, Universidade Federal de São Carlo.
[10] J.C. Castro UFSCar, 1990. Ph. D. Thesis, Universidade Federal de São Carlos.
[11] W.D. Kingery, John Wiley & Sons, 1976, pp. 71–87.
[12] S. Nascimento Silva, et al., UNITECR 93 Congress, São Paulo, Brazil, 1993, pp. 1365–1371.